

A parameter calibration method for PFC simulation: Development and a case study of limestone

Z.H. Xu^{1,2,3a}, W.Y. Wang^{1,2b}, P. Lin^{*1}, Y. Xiong^{1,2c}, Z.Y. Liu^{**1} and S.J. He^{1d}

¹Geotechnical and Structural Engineering Research Center, Shandong University, Jinan, Shandong 250061, China

²School of Qilu Transportation, Shandong University, Jinan, Shandong 250061, China

³SinoProbe Center - China Deep Exploration Center, Chinese Academy of Geological Sciences, Beijing 100037, China

(Received April 8, 2020, Revised May 31, 2020, Accepted June 1, 2020)

Abstract. The time-consuming and less objectivity are the main problems of conventional micromechanical parameters calibration method of Particle Flow Code simulations. Thus this study aims to address these two limitation of the conventional “trial-and-error” method. A new calibration method for the linear parallel bond model (CM-LPBM) is proposed. First, numerical simulations are conducted based on the results of the uniaxial compression tests on limestone. The macroscopic response of the numerical model agrees well with the results of the uniaxial compression tests. To reduce the number of the independent micromechanical parameters, numerical simulations are then carried out. Based on the results of the orthogonal experiments and the multi-factor variance analysis, main micromechanical parameters affecting the macro parameters of rocks are proposed. The macro-micro parameter functions are ultimately established using multiple linear regression, and the iteration correction formulas of the micromechanical parameters are obtained. To further verify the validity of the proposed method, a case study is carried out. The error between the macro mechanical response and the numerical results is less than 5%. Hence the calibration method, i.e., the CM-LPBM, is reliable for obtaining the micromechanical parameters quickly and accurately, providing reference for the calibration of micromechanical parameters.

Keywords: discrete element method; particle flow code; parallel bond model; micromechanical parameters; calibration method

1. Introduction

Particle Flow Code (PFC) method is one of the widely used discrete element methods in geomechanics, put forward jointly by American scholars, Cundall and Strack (1979). Compared with the continuum mechanics-based numerical approach (Lin *et al.* 2019, Xu *et al.* 2020a), the basic idea of PFC is that material is discretized into a set of rigid particles, the motion of particles is controlled by Newton's second law, and the contact force between particles is controlled by the law of force-displacement. Particles can be separated, which makes PFC capable to simulate large deformation of materials (Bock and Prusek 2015, Guo *et al.* 2020). As a discontinuous medium

calculation method, it shows good applicability in geotechnical engineering related calculation (Gracia *et al.* 2019, Hashemi *et al.* 2014, Meidani *et al.* 2018, Xu *et al.* 2020c). To characterize the rock materials or the rock-like materials, the bond model was proposed. In literature, the bond model is widely used to simulate the mechanical and failure behaviors of the rock under two dimensional conditions (Haeri *et al.* 2019, Jafri and Yoo 2018, Manouchehrian *et al.* 2014). A large number of laboratory tests and numerical simulation were conducted using linear parallel bond model, i.e., LPBM (De Silva and Ranjith 2020, Haeri *et al.* 2019, Mehranpour *et al.* 2018, Shemirani *et al.* 2018), which explain the evolution of the force chain and cracks that are difficult to observe in laboratory tests from the microscopic perspective (Hasanpour *et al.* 2016, Lotidis *et al.* 2019, Sarfarazi *et al.* 2018). The energy can be consumed by bond crack propagation or stored in the PFC model, thus the mechanism of rock failure can be further interpreted (Hofmann *et al.* 2016, Khazaei *et al.* 2015, Poulsen *et al.* 2018). It is known that the reliable selection of input parameters is the basis of successful numerical simulation (Xu *et al.* 2020b). Thus, in the above research, determining the micromechanical parameters is the precondition for effective and accurate simulation.

However, the micromechanical parameters are not directly corresponding to the macroscopic parameters of real material. The conventional mechanical parameters calibration is the “trial-and-error” process with less objectivity and much uncertainties (Chen *et al.* 2019). It

*Corresponding author, Ph.D.

E-mail: sddxytlp@163.com

**Corresponding author, Ph.D.

E-mail: liuzhy_2011@163.com

^aProfessor, Ph.D.

E-mail: zhenhao_xu@sdu.edu.cn

^bPh.D. Student

E-mail: sduwwy@163.com

^cPh.D. Student

E-mail: xiongyue19950315@163.com

^dPh.D. Student

E-mail: 942530425@qq.com

means that the conventional mechanical parameter calibration is a time-consuming process. Thus, how to obtain credible micromechanics parameters quickly is an unavoidable and important problem (Ajamzadeh *et al.* 2018). Because the parameters between particles are difficult to be determined directly by laboratory or field tests, some scholars have carried out research on the relationship between macro and micro parameters, trying to find out the law of how the micromechanical parameters influence macroscopic parameters. In literature, a series of semiquantitative function relations between micromechanical parameters and macroscopic parameters were proposed (Shi *et al.* 2019).

In order to calibrate the micromechanical parameters of the parallel bond model, enumeration method is widely used in rock micromechanical parameter calibration. It assumes a set of random micromechanical parameters and adopts them to carry out numerical tests. If the elastic modulus, uniaxial compressive strength and Poisson's ratio are in agreement with the laboratory test results, the micromechanical parameters can be accepted. Its core idea is to reproduce the macroscopic mechanical response of rock by iterating the micromechanical parameters through so-called "trial-and-error" process. Generally, researchers carry out laboratory tests to obtain the uniaxial compressive strength, elastic modulus and Poisson's ratio of rocks. For example, Bahaaddini *et al.* (2013) applied numerical program of uniaxial compression test to calibrate the micromechanical parameters according to the order of macro-elastic modulus, Poisson's ratio and uniaxial compressive strength of rocks. It was supposed that the macroscopic modulus of elasticity was controlled by effective modulus, stiffness ratio, parallel bond modulus and parallel bond stiffness ratio. In addition, Poisson's ratio was controlled by the microscopic stiffness parameter. The uniaxial compressive strength was decided by the microscopic strength parameter of the parallel bond. After many attempts, a set of micromechanical parameters were obtained. In the process of micromechanical parameters calibration, the particle density had no effect on the quasi-static behavior of the model (Bahaaddini *et al.* 2016). The traditional calibration method depends on the process of enumeration to select the micromechanical parameters to reproduce the desired macro properties measured in the laboratory experiments, which has less objectivity and much uncertainties. From the practical experiences, for instance, the microscopic stiffness ratio affects all the values of macro elastic modulus, Poisson's ratio and uniaxial compressive strength. If the Poisson's ratio is calibrated against stiffness ratio, the elastic modulus and the uniaxial compressive strength will be changed by the variance of the stiffness ratio. Furthermore, it is known that the number of input parameters of linear parallel bond model is more than 10, which makes it more difficult to calibrate the micromechanical parameters using enumeration method.

The present study is focused on determining the micromechanical parameters of the rock material through a quick process. Firstly, a series equations are proposed to reduce the number of independent micromechanical parameter. Then, the semi-quantitative functional

relationship between the macroscopic parameters and the micromechanical parameters are obtained based on multi-factor variance analysis and the multiple linear regression. Furthermore, the micromechanical parameter correction iteration formula is proposed through the single factor analysis. Hence, a quick calibration method of linear parallel bond model (CM-LPBM) is developed, and the micromechanical parameter calibration of the limestone is taken as an case to verify the proposed method. It provides guidance for determining the micromechanical parameters of limestone based on parallel bond model reasonably and quickly. In addition, the CM-LPBM is compared with laboratory tests and other calibration methods.

2. Selection and simplification of micromechanical parameters of limestone

When PFC method is used to simulate the mechanical behavior of rock and soil, the commonly used contact constitutive models include linear model (LM), linear contact bond model (LCBM) and linear parallel bond model (LPBM). LM and LCBM are suitable for simulating soil materials (Cundall and Strack 1979, Kwok and Bolton 2010). Compared with contact bonds, parallel bonds can transmit both force and moment, which can well reflect the mechanical properties of rock and hence has been widely applied to numerical simulation of intact and fractured rock masses (Bahrani and Kaiser 2017). Thus, the LPBM was adopted to simulate the mechanical behavior of rock in this paper. When the parallel bond breaks, the unbonded model is equivalent to the linear contact model. The parallel bond contact breakages can be regarded as microscopic cracks, and the combination of multiple microscopic cracks will evolve into a macro-fracture of the rock.

The linear parallel bond model was applied in this study to establish the 2D discrete element numerical model of rock. The model-generation procedure refers to the fistPkg26 (Potyondy, 2018). The size of specimens was 100 mm in height and 50 mm in width (see in Fig. 1), and the procedure of model generation consists of a packing phase followed by a finalization phase. In the packing phase, the linear contact model was installed at all grain-grain contacts and the PFC walls were generated to prevent the balls escaping from the vessel. Additionally, the movement of the vessel walls was controlled by the servomechanism. Subsequently, in the finalization phase, the linear parallel bond model and the LPBM related material properties were assigned to the contacts. Ultimately, the well-connected ball assembly was obtained.

The micromechanical parameters and physical parameters of the model shall be input when uniaxial compression test is carried out to calibrate the micromechanical parameters of limestone. Micromechanical parameters include effective modulus E^* , stiffness ratio κ^* , frictional coefficient μ , parallel bond effective modulus \bar{E}^* , parallel bond stiffness ratio $\bar{\kappa}^*$, mean value of parallel bond normal strength $\bar{\sigma}_{c,m}$, mean value of parallel bond tangential strength $\bar{\tau}_{c,m}$, standard deviation of parallel bond normal strength $\bar{\sigma}_{c,sd}$, standard deviation of parallel bond tangential strength $\bar{\tau}_{c,sd}$, and radius multiplier $\bar{\lambda}$.

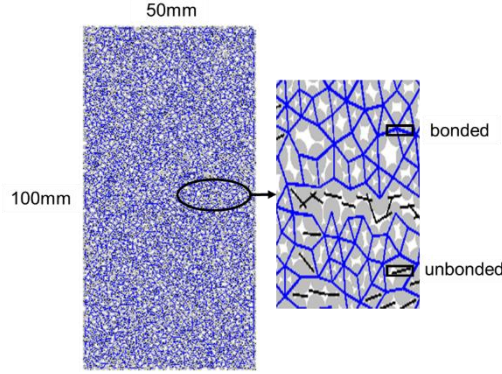
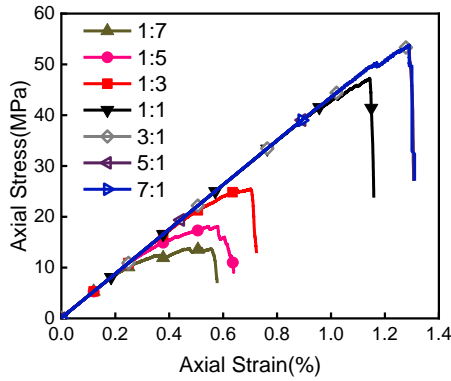
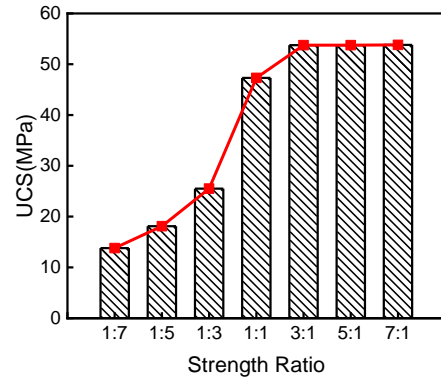


Fig. 1 Numerical sample established in present research



(a) Stress-strain curves with different bond strength ratios



(b) Uniaxial compressive strength of numerical models with different bond strength ratios

Fig. 2 Influence of bond strength ratio on macroscopic mechanical response

Table 1 Values of micromechanical parameters

Micromechanical parameter	E^* /GPa	κ^*	$\bar{\sigma}_{c,m}$ /MPa	$\bar{\sigma}_{c,sd}$ /MPa	$\bar{\tau}_{c,m}$ /MPa	$\bar{\tau}_{c,sd}$ /MPa	μ
Value	3	3	26.5	6.625	132.5	33.125	0.7

Table 2 Comparison between indoor tests and numerical test

Serial No.	H /mm	W /mm	ρ /kg·m ⁻³	E /GPa	σ_{UCS} /MPa	ν
a1	98.08	49.35	2700	3.84	49.67	-
a2	96.44	49.38	2680	4.07	52.97	-
a3	99.56	49.55	2700	4.21	56.72	-
Mean value	-	-	-	4.04	53.12	0.250
Numerical test	100	50	2700	4.09	53.75	0.251
Relative error	-	-	-	1.25%	1.19%	0.40%

Physical parameters include minimum particle size R_{min} , maximum particle size R_{max} , particle density ρ , rock specimen height H and rock specimen width W . Macroscopic parameters to be obtained are elastic modulus E , Poisson's ratio ν and uniaxial compressive strength σ_{UCS} . With relatively large number of the input parameters, the model parameters are therefore simplified to reduce the variation of the parameters.

Previous studies by Potyondy and Cundall (2004) provide a fundamental reference to simplify the

micromechanical parameters. It shows that when $E^* = \bar{E}^*$, $\kappa^* = \bar{\kappa}^*$, $\bar{\lambda} = 1$, $R_{max}/R_{min} = 1.66$ are satisfied, the PFC numerical test results can reproduce the characteristics of rock materials. Additionally, the standard deviation of the parallel bond strength is assigned as a quarter of the parallel bond strength in the subsequent study. The input micromechanical parameters will satisfy the above relations.

The particle sizes relative to model sizes will affect model accuracy and macroscopic characteristics, therefore, it is necessary to determine a reasonable particle size to ensure the model accuracy and calculation efficiency. When the particle size is very small, its influence on the macroscopic characteristics of the model can be ignored, but the model size and computer performance contradict each other, so the particle size cannot be too small. The R_{max}/R_{min} is regarded as a set value. To determine R_{min} , the resolution of a dimension RES (Zhou *et al.* 2011) is defined as:

$$RES = (L/R_{min})[1/(1 + R_{max}/R_{min})] \quad (1)$$

where L is the minimum size of the model. Zhou (2011) carried out PFC uniaxial compression numerical experiment to study the influence of RES on macroscopic parameters of rock and soil materials. The results showed that the number and size of particles had little effect on macro mechanical parameters when $RES \geq 10$ and RES was taken as 10 in the follow-up study. Combined with previous

research, this paper found that when R_{min} was 0.5 mm, its RES is more than 10, which can satisfy the accuracy requirement of the model and avoid the problems caused by size effect.

Previous research showed that ratio of parallel bond strength mean value $\bar{\tau}_{c,m}/\bar{\sigma}_{c,m}$ had an impact on the macroscopic mechanical response of the numerical specimen. Uniaxial compressive numerical tests were carried out with different $\bar{\tau}_{c,m}/\bar{\sigma}_{c,m}$. Stress strain curves and uniaxial compressive strength σ_{UCS} obtained are shown in Fig. 2(a) and Fig. 2(b) respectively. It can be seen that the specimen exhibits brittleness when $\bar{\tau}_{c,m}/\bar{\sigma}_{c,m} \geq 1/3$. We note that the slope of stress-strain curve nearly kept constant when $\bar{\tau}_{c,m}/\bar{\sigma}_{c,m}$ changed. The uniaxial compressive strength σ_{UCS} increased with the increase of the ratio of the mean value of parallel bond strength $\bar{\tau}_{c,m}/\bar{\sigma}_{c,m}$. However, the macroscopic mechanical parameters of rock had little change when $\bar{\tau}_{c,m}/\bar{\sigma}_{c,m} > 2$, the reason is that the uniaxial compressive strength of numerical model was controlled by $\bar{\sigma}_{c,m}$ under this condition. In literature, the mean strength ratio can be set to 5 to simulate the mechanical behavior of rock, and the obtained simulation results were good consistent with the laboratory tests (Li *et al.* 2016, Fakhimi 2004). Therefore, in present study, the mean strength ratio $\bar{\tau}_{c,m}/\bar{\sigma}_{c,m}$ is set to a constant value equal to 5. The four micromechanical parameters ($\bar{\sigma}_{c,m}$, $\bar{\tau}_{c,m}$, $\bar{\sigma}_{c,sd}$, $\bar{\tau}_{c,sd}$) related to parallel bond strength are finally simplified into a free variable ($\bar{\sigma}_{c,m}$).

To verify the rationality of the parameter simplification analysis, numerical simulation was conducted. It was set that $E^* = \bar{E}^*$, $\kappa^* = \bar{\kappa}^*$, $\bar{\lambda} = 1$, $R_{min} = 0.5$ mm, $R_{max}/R_{min} = 1.66$, $\bar{\sigma}_{c,sd} = 0.25\bar{\sigma}_{c,m}$, $\bar{\tau}_{c,sd} = 0.25\bar{\tau}_{c,m}$, $\bar{\tau}_{c,m}/\bar{\sigma}_{c,m} = 5$. The uniaxial compression test results regarding limestone of karst conduit in Qiyueshan Tunnel (Wu 2017) was taken as the target. It is found that the independent micromechanical parameters in the parallel bond contact constitutive model are simplified to E^* , κ^* , $\bar{\sigma}_{c,m}$ and μ . The numerical experiment of PFC^{2D} uniaxial compression was carried out by means of “trial-and-error method”. Based on the iterative process of “trial-and-error method” reported by Bahaaddini *et al.* (2013), the macroscopic parameters including E , ν and σ_{UCS} were matched by enumeration of the micromechanical parameters in order. After many times’ attempts, the micromechanical parameters were obtained. The selected micromechanical parameters are shown in Table 1. The stress-strain curves obtained from laboratory uniaxial compression tests and numerical tests are shown in Fig. 3. The results of numerical and laboratory tests are compared and the relative errors are shown in Table 2. From the table, the relative error of the numerical test is not more than 1.25%, which guarantees the accuracy of the established model. It can be seen that the macroscopic responses of the numerical model are in good agreement with laboratory test. Thus the validity of the simplification of the micromechanical parameters in the present study is verified. In the following study, we select the micromechanical parameters shown in Table 1 as the benchmark, referred to as “benchmark parameters”.

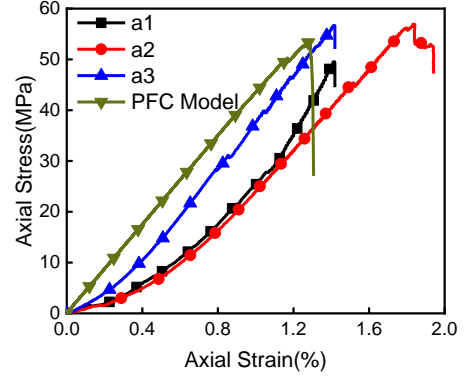


Fig. 3 Numerical model and test result comparison

3. Macro-and-micro parameter function relationship based on multiple linear regression

3.1 Multi-factor variance analysis

Elastic modulus E , Poisson’s ratio ν and uniaxial compressive strength σ_{UCS} can be obtained through uniaxial compression numerical test so as to study the effect of micromechanical parameters ($E^*, \kappa^*, \mu, \bar{E}^*, \bar{\kappa}^*, \bar{\sigma}_{c,m}, \bar{\tau}_{c,m}, \bar{\sigma}_{c,sd}, \bar{\tau}_{c,sd}, \bar{\lambda}$) on macroscopic parameters. Using the above parameters to simplify the method, set dependent variables to be E^* , κ^* , $\bar{\sigma}_{c,m}$ and μ , take parameters in Table 1 as the benchmark, and carry out orthogonal numerical experiment with 4 factors and 5 levels by means of the $L_{25}(5^4)$ orthogonal table. The orthogonal experiment and simulation results are shown in Table 3.

Based on the orthogonal test results shown in Table 3, multivariate analysis of variance is carried out to analyze the main effects of various factors. This paper adopts F-test with the significant level α being 0.05. If $\text{Sig.} < 0.05$, it is considered that corresponding micromechanical parameters have a significant effect on the macroscopic parameters. The results are shown in Fig. 4.

Table 3 Orthogonal experimental design

Scenarios	E^* /GPa	κ^*	$\bar{\sigma}_{c,m}$ /MPa	μ	E /GPa	ν	σ_{UCS} /MPa
1	2	2	21.5	0.8	3.21	0.217	45.98
2	5	1	21.5	0.6	8.62	0.128	42.00
3	4	1	26.5	0.7	7.23	0.104	54.79
4	1	2	26.5	0.9	1.80	0.196	74.80
5	3	1	31.5	0.8	5.63	0.109	68.31
6	2	3	31.5	0.7	2.89	0.244	69.25
7	4	2	36.5	0.6	5.79	0.215	79.71
8	5	2	31.5	0.5	7.18	0.213	53.36
9	5	4	26.5	0.8	6.11	0.276	44.70
10	4	4	31.5	0.9	4.97	0.273	55.10
11	3	4	36.5	0.5	3.78	0.272	65.40

Table 3 Continued

Scenarios	E^* /GPa	κ^*	$\bar{\sigma}_{c,m}$ /MPa	μ	E /GPa	ν	σ_{UCS} /MPa
12	2	4	16.5	0.6	2.67	0.273	32.30
13	2	1	36.5	0.9	3.97	0.097	96.93
14	4	3	21.5	0.5	5.22	0.250	43.07
15	1	3	36.5	0.8	1.62	0.233	98.86
16	1	1	16.5	0.5	2.14	0.125	59.34
17	3	2	16.5	0.7	4.64	0.196	35.46
18	5	5	36.5	0.7	5.36	0.304	60.86
19	1	4	21.5	0.7	1.51	0.255	50.44
20	3	5	21.5	0.9	3.62	0.288	39.97
21	2	5	26.5	0.5	2.47	0.288	49.29
22	4	5	16.5	0.8	4.63	0.297	27.54
23	5	3	16.5	0.9	6.33	0.245	31.64
24	1	5	31.5	0.6	1.42	0.273	67.39
25	3	3	26.5	0.6	4.14	0.252	54.43

According to the results of multivariate analysis of variance, the significant influence order of macroscopic parameters obtained is as follows:

Elastic modulus E : factors with significance include effective modulus E^* and stiffness ratio κ^* , besides $E^* > \kappa^*$;

Poisson's ratio ν : factor with significance is stiffness ratio κ^* only;

Uniaxial compressive strength σ_{UCS} : factors with significance include effective modulus E^* , stiffness ratio κ^* and parallel bond normal strength mean value $\bar{\sigma}_{c,m}$, besides $\bar{\sigma}_{c,m} > E^* > \kappa^*$.

Furthermore, frictional coefficient μ has no significant influence on macroscopic parameters in present study. Parallel bond strength has no significant influence on the macroscopic elastic parameters, corroborated with the influence of parallel bond strength parameters on macroscopic elastic parameters revealed in Fig. 2 above. Uniaxial compressive strength is mainly affected by the parameter of parallel bond strength. In addition, it should be noted that the microscopic stiffness parameters also have a significant effect on macroscopic uniaxial compressive strength.

3.2 Regression analysis of macro-and-micro parameters based on multi-factor variance analysis

Based on the results of multivariate analysis of variance, the macro-micro parametric function was established step by step according to the number of significant factors.

Since the stiffness ratio κ^* is the only micromechanical parameter that has a significant effect on Poisson's ratio ν , the method of controlling variables can be adopted. Based on the micromechanical parameters shown in Table 1, a

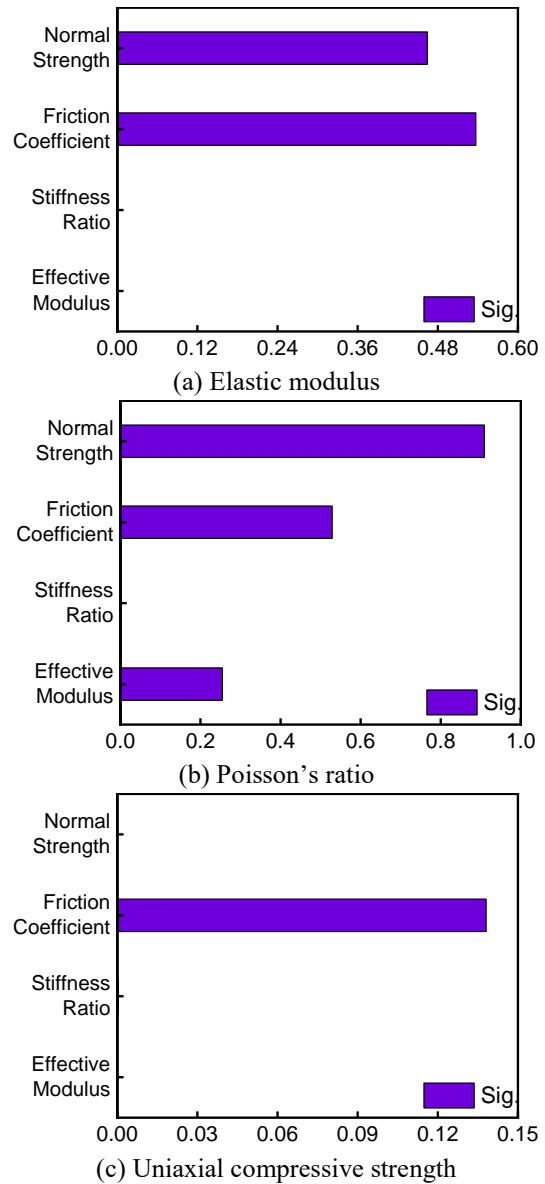


Fig. 4 Results of multi-factor variance analysis

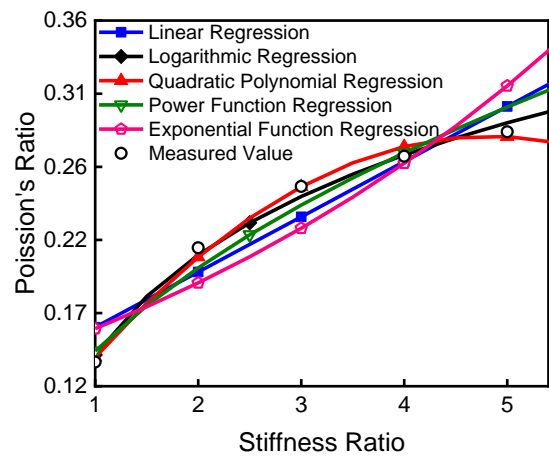


Fig. 5 Comparison of the stiffness ratio -Poisson's ratio curves by different regression methods

series of numerical uniaxial compressive tests were carried

out with different stiffness ratios κ^* . The ν - κ^* curves obtained by different regression methods are shown in Fig. 5.

It is can be seen that although it is convenient to use linear regression, the single linear function does not have enough precision to describe the functional relationship between Poisson's ratio and stiffness ratio ($R^2 = 0.8997$); considering significance level and coefficient of determination, a logarithmic relation is used to describe the effect of stiffness ratio on Poisson's ratio ($R^2 = 0.9916$, Sig. = 0.00033), which is more precise. Its function relation is as follows:

$$\nu = 0.095 \ln \kappa^* + 0.141 \quad (R^2 = 0.9916) \quad (2)$$

For elastic modulus E , factors with significant effect include effective modulus E^* and stiffness ratio κ^* . Using multiple linear regression, the function relation is as follows:

$$E = 1.257E^* - 0.475\kappa^* + 1.933 \quad (R^2 = 0.963) \quad (3)$$

For uniaxial compressive strength σ_{UCS} , factors with significant effect include effective modulus E^* , stiffness ratio κ^* and parallel bond normal strength mean value $\bar{\sigma}_{c,m}$, the function relation is shown in Eq.(4):

$$\sigma_{UCS} = -5.402E^* - 3.880\kappa^* + 2.092\bar{\sigma}_{c,m} + 28.454 \quad (R^2 = 0.922) \quad (4)$$

From the function relation of macro-micro parameters, the positive and negative correlations between macroscopic parameters and micromechanical parameters can be obtained. Poisson's ratio ν is positively related to stiffness ratio κ^* ; elastic modulus E is positively related to effective modulus E^* and negatively related to stiffness ratio κ^* ; uniaxial compressive strength σ_{UCS} is positively related to parallel bond normal strength mean value $\bar{\sigma}_{c,m}$ and negatively related to effective modulus E^* and stiffness ratio κ^* .

4. Micromechanical parameter calibration method and case study

4.1 Micromechanical parameter inversion method

Based on the macro-micro parameter function relation, calibration formula of micromechanical parameters can be obtained by back calculation, shown as Eqs. (5)-(7):

$$\kappa^* = e^{(\nu-0.141)/0.095} \quad (5)$$

$$E^* = (E + 0.475\kappa^* - 1.933)/1.257 \quad (6)$$

$$\bar{\sigma}_{c,m} = (\sigma_{UCS} + 5.402E^* + 3.880\kappa^* - 28.454)/2.092 \quad (7)$$

During PFC micromechanical parameter calibration, macro-mechanical parameters (uniaxial compressive σ_{UCS} , elastic modulus E and Poisson's ratio ν) shall be obtained first from uniaxial compressive tests and then calculate micromechanical parameters preliminarily by Eqs. (5), (6) and (7) as the remaining micromechanical parameters

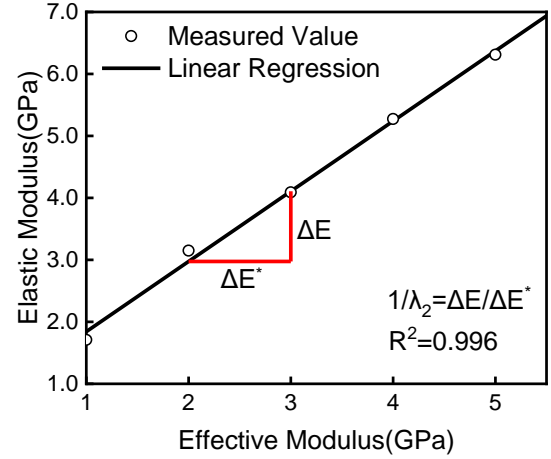


Fig. 6 Influence curve of effective modulus on elastic modulus

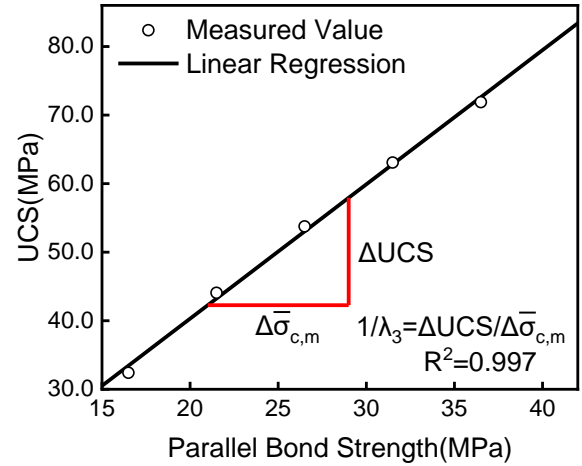


Fig. 7 Influence curve of parallel bond normal strength on uniaxial compressive strength

satisfy the simplified parameter relations above; carry out PFC numerical tests with this group of micromechanical parameters to calculate the macroscopic parameters; compare the macroscopic parameters obtained from numerical tests and macroscopic responses obtained from laboratory test. If the calibration accuracy does not meet the requirements, then the micromechanical parameters are adjusted iteratively until the reasonable accuracy range is reached.

In order to determine the iteration step, numerical tests of single factor effect of effective modulus on elastic modulus and parallel bond normal strength on uniaxial compressive strength were carried out by controlling variables. Univariate function curve obtained are shown in Figs. 6 and 7. It can be seen that the two sets of micromechanical parameters are positively related to corresponding macroscopic parameters and have significant effect on macroscopic parameters, which is consistent with the results obtained by multi-factor variance analysis and regression analysis. It is reasonable to conduct iterative adjustment to the micromechanical parameters by linear function.

Macroscopic parameters such as uniaxial compressive

strength σ_{UCS} , elastic modulus E and Poisson's ratio ν can be obtained by laboratory physical tests. On the basis of ensuring that conditions like boundary and loading are consistent with physical tests, the PFC parameter calibration numerical tests can be carried out. According to the principle that PFC simulation shall be consistent with the macroscopic responses of physical experiments, the micromechanical parameters of the constitutive model of parallel bond contact should be determined. The calibration of limestone is then taken as an example, and its specific process is as follow:

1) Following the principle that the size of numerical test model shall be consistent with the size of laboratory physical test rock samples, the height H and width W of rock samples are obtained, therein, the recommended height H and width W being 100 mm and 50 mm respectively in the present study. Measure and calculate the particle density ρ . Carry out laboratory tests to obtain the macro-mechanical parameters including uniaxial compressive strength σ_{UCS} , elastic modulus E and Poisson's ratio ν .

2) Determine minimum particle size R_{min} and maximum particle size with comprehensive consideration of simulation preciseness, calculation efficiency and particle size distribution of rock samples. As is hard to obtain real particle distribution size, the particle size can be simplified to Gauss distribution. The number of the shortest edge particles should be greater than 30; moreover, the RES of the model calculated based on Eq. (1) shall be no less than 10, therefore, it is suggested that $R_{min} = 0.5$ mm, $R_{max}/R_{min} = 1.66$.

3) Preliminary calibration of elastic parameters, including elastic modulus E and Poisson's ratio ν . The micromechanical parameter, stiffness ratio κ^* is obtained by substituting Poisson's ratio ν obtained from laboratory tests into Eq. (5); the micromechanical parameter, effective modulus E^* is obtained by submitting elastic modulus E and stiffness ratio κ^* into Eq. (6).

4) Preliminary calibration of strength parameter, i.e., uniaxial compressive strength σ_{UCS} . Mean value of parallel bond normal strength $\bar{\sigma}_{c,m}$ is obtained by submitting uniaxial compressive strength σ_{UCS} , stiffness ratio κ^* and effective modulus E^* into Eq. (7).

5) Set $E^* = \bar{E}^*$, $\kappa^* = \bar{\kappa}^*$, $\bar{\lambda} = 1$, $\bar{\sigma}_{c,sd} = 0.25\bar{\sigma}_{c,m}$, $\bar{\tau}_{c,sd} = 0.25\bar{\tau}_{c,m}$, $\bar{\tau}_{c,m} = 5\bar{\sigma}_{c,m}$, and all micromechanical parameters can be obtained;

6) Input the above micromechanical parameters to PFC^{2D} and carry out PFC parameter calibration numerical tests to obtain the macroscopic responses of numerical model. Compare the macroscopic parameters of the numerical model with that of the physical tests and calculate the error. Take allowable error as 5%. Accept the calibrated micromechanical parameters if the relative error is less than or equal to 5%, otherwise, micromechanical parameter correction iteration is needed.

Based on the influence of the micromechanical parameters on the macroscopic parameters revealed above, micromechanical parameters can be calibrated iteratively according to the order of stiffness ratio, effective modulus and parallel bond normal strength, which can effectively reduce the influence of the posterior calibration on the

macroscopic parameters of the prior order calibration. Micromechanical parameter correction method based on linear function iteration can be obtained and the specific iteration procedure is as follows:

1) Calculate the relative error of Poisson's ratio ν between the numerical model and the laboratory experimental model. Accept the value of stiffness ratio if its relative error is no more than 5%; conduct iterative calibration to stiffness ratio κ^* if the relative error of Poisson's ratio is greater than 5% and the iterative function is shown in Eq. (8),

$$\kappa^{*(k+1)} = \kappa^* + \lambda_1 \times \text{sgn}(\Delta\nu^{(k)}) \quad (8)$$

$$\text{sgn}(\Delta\nu^{(k)}) = \begin{cases} 1 & \Delta\nu^{(k)} \geq 0 \\ -1 & \Delta\nu^{(k)} < 0 \end{cases} \quad (9)$$

where $\Delta\nu^{(k)}$ is the difference value between the actual Poisson's ratio and the Poisson's ratio obtained from numerical model in No. k iteration, and λ_1 is the correction step of stiffness ratio. Because of the convenience of linear function, the stiffness ratio was corrected by using linear function. Suggested λ_1 in the present study is 0.1 and “+” indicates a positive correlation between Poisson's ratio and stiffness ratio.

$$|\Delta\nu^{(k)}/\nu| \leq 0.05 \quad (10)$$

Adopt the Eq. (8) to iterate with equal step length and carry out numerical experiments to verify. The termination condition of iteration is shown in Eq. (10). Accept the correction value of stiffness ratio κ^* after meeting the termination condition of iteration and complete the calibration of stiffness ratio κ^* .

2) Set stiffness ratio κ^* as $\kappa^{*(k)}$ and keep other micromechanical parameters unchanged. Calculate the relative error of elastic modulus between numerical model and laboratory model; accept the value of effective modulus E^* if the relative error is no greater than 5%; otherwise, conduct iterative calibration to effective modulus E^* . And the iteration formula is shown in Eq. (11):

$$E^{*(k+1)} = E^* + \lambda_2 \times \Delta E^{(k)} \quad (11)$$

where $\Delta E^{(k)}$ is the difference value between the actual elastic modulus and the elastic modulus obtained from numerical model in No. k iteration and λ_2 is the iteration coefficient of effective modulus. It can be seen that the λ_2 is the reciprocal value of slope of the curve in Fig. 6. Additionally, it is reasonable to conduct correction to effective modulus by adopting linear iteration formula ($R^2 = 0.996$). Suggested λ_2 in the present study is 0.883 and “+” indicates a positive correlation between elastic modulus and effective modulus.

$$|\Delta E^{(k)}/E| \leq 0.05 \quad (12)$$

Adopt the Eq. (11) to correct E^* and carry out numerical experiments to verify. The termination condition of iteration is shown in Eq. (12). Accept the correction value of effective modulus E^* after meeting the termination condition of iteration and complete the calibration of effective modulus E^* .

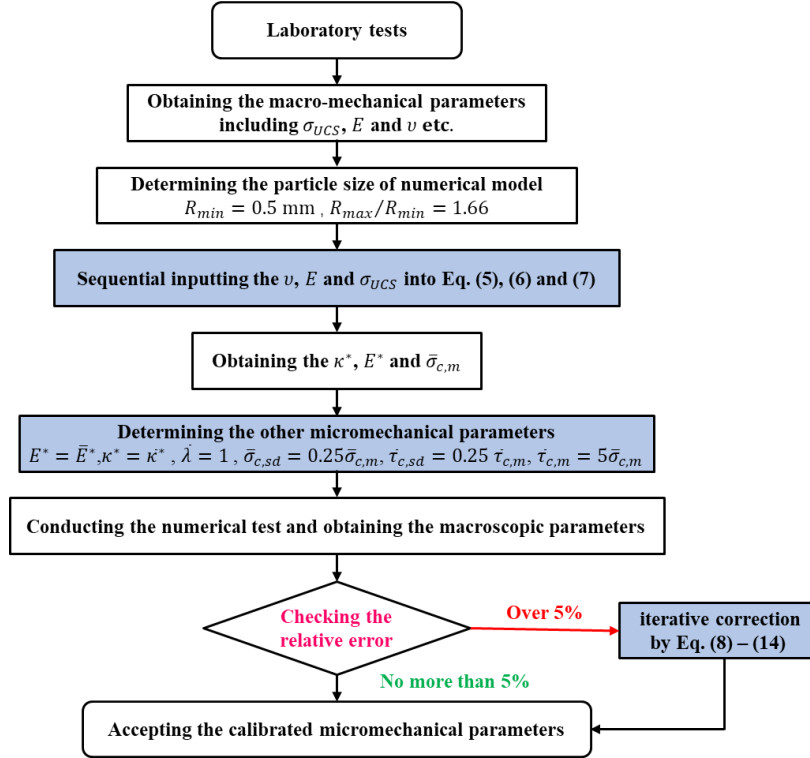


Fig. 8 Procedure of the proposed mechanical parameters calibration method (CM-LPBM)

Table 4 The target macroscopic mechanical parameters of limestone

σ_{UCS}/MPa	E/GPa	ν
80.23	20.20	0.262

Table 5 The obtained macroscopic mechanical parameters of limestone using CM-LPBM

Iterative number	Micromechanical parameter				The obtained macro-parameter					
	κ^*	E^*/GPa	$\bar{\sigma}_{c,m}/\text{MPa}$	μ	ν	$\varepsilon_\nu/\%$	E/GPa	$\varepsilon_E/\%$	σ_{UCS}/MPa	$\varepsilon_{\sigma_{UCS}}/\%$
Target					0.262	20.20	80.23			
Step1	3.57	15.88	72.38	0.7	0.256	2.3	16.78	16.9	104.44	30.2
Step2	3.57	18.90	72.38	0.7	0.261	0.4	19.52	3.4	89.25	11.2
Step3	3.57	18.90	67.77	0.7	0.254	3.1	19.57	3.1	83.5	4.1

3) Adopt the corrected stiffness ratio κ^* and corrected effective modulus E^* and keep other micromechanical parameters unchanged. Calculate the relative error of uniaxial compressive strength between numerical model and laboratory experiment model. Accept the value of parallel bond normal strength $\bar{\sigma}_{c,m}$ if its relative error is no greater than 5%; otherwise, conduct iterative calibration to parallel bond normal strength $\bar{\sigma}_{c,m}$ and its iteration formula is shown in Eq. (13):

$$\bar{\sigma}_{c,m}^{(k+1)} = \bar{\sigma}_{c,m} + \lambda_3 \times \Delta\sigma_{UCS}^{(k)} \quad (13)$$

where $\Delta\sigma_{UCS}^{(k)}$ is the difference value between the actual uniaxial compressive strength and the uniaxial compressive strength obtained from numerical model in No. k iteration and λ_3 is the iteration coefficient of parallel bond normal

strength. The λ_3 can be calculated in the same way as λ_2 . As shown in Fig. 7, the suggested value of λ_3 is 0.511; “+” indicates a positive correlation between uniaxial compressive strength and parallel bond normal strength.

$$|\Delta\sigma_{UCS}^{(k)}/\sigma_{UCS}| \leq 0.05 \quad (14)$$

Adopt the step length λ_3 in Eq. (13) to correct $\bar{\sigma}_{c,m}$ and carry out numerical experiments to verify. The termination condition of iteration is shown in Eq. (14). Accept the correction value of parallel bond normal strength $\bar{\sigma}_{c,m}$ after meeting the termination condition of iteration and complete the calibration of parallel bond normal strength $\bar{\sigma}_{c,m}$.

Finally, the micromechanical parameters corresponding to macroscopic mechanical parameters of laboratory rock samples are calibrated, and the procedure of the proposed CM-LPBM can be seen in Fig. 8.

4.2 Case study

In order to verify the micromechanical parameter calibration method (CM-LPBM) proposed in the present study, we have obtained the limestone samples from the pit of Huarun Cement (Pingnan) Co., Ltd. Hejing Phase I and Phase II limestone mine and carried out uniaxial compression tests. The cylindrical specimen is obtained with the height being 100 mm and the width 50 mm. The mechanical parameters obtained are shown in Table 4. We then select the macroscopic parameters in Table. 4 for micromechanical parameter calibration.

Calibrate the micromechanical parameters of limestone by adopting the proposed calibration method (see in Fig. 8), and specific calibrating procedures are as follows:

Step 1: Carry out experiment tests with the height, width

and density of rock specimen being 100 mm, 50 mm and 2680 kg/m³ respectively. From the obtained data, rock uniaxial compressive strength σ_{UCS} is 80.23 MPa, elastic modulus E is 20.20 GPa and Poisson's ratio ν is 0.262;

Step 2: Set the minimum particle radius $R_{min}=0.5$ mm and $R_{max}/R_{min}=1.66$, and particle distribution follows Gauss distribution;

Step 3: Preliminary calibration of elastic parameters of limestone. Submit the Poisson's ratio of limestone $\nu=0.262$ obtained from laboratory tests into Eq. (5) and obtain the stiffness ratio $\kappa^*=3.57$. Submit limestone elastic modulus $E=20.20$ GPa and stiffness ratio $\kappa^*=3.57$ into Eq. (6) and obtain the effective modulus $E^*=15.88$ GPa;

Step 4: Preliminary calibration of limestone strength parameter, uniaxial compressive strength σ_{UCS} . Submit uniaxial compressive strength $\sigma_{UCS}=80.23$ MPa, stiffness ratio $\kappa^*=3.57$ and effective modulus $E^*=15.88$ GPa into Eq. (7) and obtain the mean value of parallel bond normal strength $\bar{\sigma}_{c,m}=72.38$ MPa.

Step 5: Set $E^*=\bar{E}^*$, $\kappa^*=\bar{\kappa}^*$, $\bar{\lambda}=1$, $\bar{\sigma}_{c,sd}=0.25\bar{\sigma}_{c,m}$, $\bar{\tau}_{c,sd}=0.25\bar{\tau}_{c,m}$, $\bar{\tau}_{c,m}=5\bar{\sigma}_{c,m}$ and $\mu=0.7$, and then obtain the remaining micromechanical parameters;

Step 6: Input the above micromechanical parameters into PFC^{2D}, establish the limestone PFC model based on LPBM and carry out uniaxial compressive numerical tests. Macroscopic responses of the numerical model can be obtained. Based on results of numerical simulation, the macroscopic elastic modulus $E=16.78$ GPa, Poisson's ratio $\nu=0.256$ and uniaxial compressive strength $\sigma_{UCS}=104.44$ MPa;

It can be seen that the relative error of Poisson's ratio ν is less than 5%, meeting the requirement of accuracy while there is relatively big error of the elastic modulus E and uniaxial compressive strength σ_{UCS} between numerical simulation and laboratory tests, which needs to be corrected by linear iteration.

Step 7: Conduct iterative correction of contact modulus. Submit $\Delta E^{(1)}=3.42$ GPa into Eq.(11) and obtain $E^{*(2)}=18.90$ GPa. Keep other parameters unchanged and conduct modulus correction only. The parameters of limestone uniaxial compressive strength $\sigma_{UCS}=89.25$ MPa, elastic modulus $E=19.52$ GPa and Poisson's ratio $\nu=0.261$ were obtained through numerical tests. Carry out accuracy verification to Poisson's ratio ν , elastic modulus E and uniaxial compressive strength σ_{UCS} with Eq. (10), (12) and (14) respectively; with calculation, apart from uniaxial compressive strength σ_{UCS} , the other macroscopic parameters all meet the accuracy requirement.

Step 8: Conduct iterative correction to parallel bond normal strength. Submit $\Delta\sigma_{UCS}^{(1)}=-9.02$ MPa into Eq. (13) and obtain $\bar{\sigma}_{c,m}^{(2)}=67.77$ MPa. Keep other parameters unchanged and correct parallel bond normal strength only. Carry out numerical tests and obtain limestone uniaxial compressive strength $\sigma_{UCS}=83.5$ MPa, elastic modulus $E=19.57$ GPa and Poisson's ratio $\nu=0.254$. Carry out accuracy verification to Poisson's ratio ν , elastic modulus E and uniaxial compressive

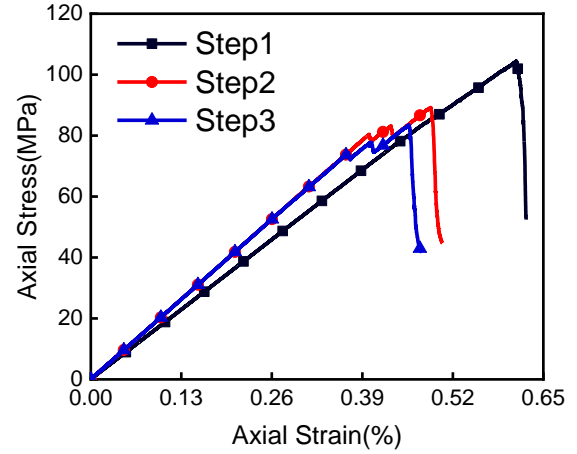


Fig. 9 Stress-strain curves obtained from the process of parameter calibration

strength σ_{UCS} with Eq. (10), (12) and (14) respectively; the specific procedure is shown in Table 5. It can be seen that the three iteration termination conditions were matched, and relative error were controlled within 5%. Thus, a set of LPBM model micromechanical parameters which can indicate macroscopic response of limestone was obtained successfully through CM-LPBM.

The stress-strain curves obtained from the process of parameter calibration can be seen in Fig. 9. It can be seen that after three steps of numerical calculations, the micromechanical parameters corresponding to the macroscopic responses of limestone in laboratory tests were obtained. We also note that there is a significant difference between the curve of Step1 and the curve of Step3.

Because it is difficult to avoid the error in preliminary calibration of micromechanical parameters by using the semi-quantitative functional relationship between micromechanical parameters and macroscopic parameters, in the second and third steps of calibration, iterative correction was conducted based on Eq. (8)-(14). It can be seen that the calibration of elastic parameters will affect the strength parameters of limestone during iteration correction, while the elastic properties of the numerical model are basically unchanged during the process of calibration of limestone strength parameters. When the parallel bond strength is adjusted, the difference at the slope of stress-strain curve can be neglected. The influence law between macroscopic and microscopic mechanical parameters reflected in the calibration process (see in Fig. 9 and Table 5) further verified the results of multi-factor variance analysis in Section 3, and the accuracy and efficiency of CM-LPBM meet the requirements of micromechanical parameter calibration.

5. Discussion

In order to further validate the proposed calibration method, i.e., CM-LPBM, other calibration methods were performed for obtaining the micromechanical parameters of limestone. Based on physical test, the macroscopic

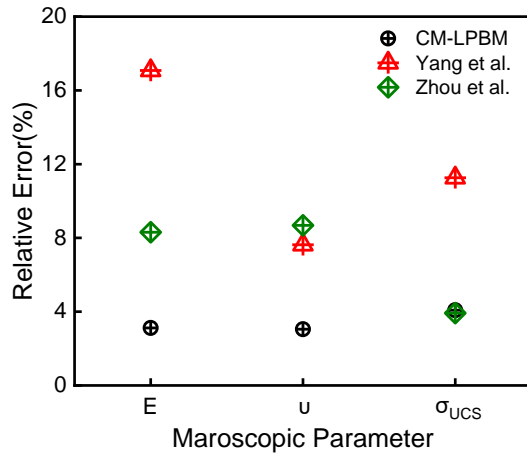


Fig. 10 Comparison of CM-LPBM and previous calibration methods

parameters of limestone are shown in Table 4. Then, the accuracy of other two methods is compared.

According to Buckingham π theorem, Yang *et al.* (2006) used PFC^{2D} to model the bonded materials and studied the quantitative relationships between particle level parameters and mechanical properties of the specimens. They got dimensionless parameters and then established the empirical formulas between macro and micro parameters, the relation is given as follows:

$$\nu = 0.20 \ln \kappa^* + 0.14 \quad (15)$$

$$\frac{E}{E^*} = 0.78 + 0.14 \ln \frac{H}{R_{avg}} - 0.34 \ln \kappa^* \quad (16)$$

$$\sigma_{UCS} / \bar{\sigma}_{c,m} = 1.69 \sim 1.88 \quad (17)$$

It should be noted that Young's modulus and Poisson's ratio are computed under plane stress state to match the properties of the real materials in Yang's study. In present study, the calculation method of the elastic constants is same as Potyondy's (2018). We obtained the micromechanical parameters using Eqs. (15)-(17), and then carried out numerical simulation to get the macroscopic parameters of limestone. The macroscopic parameters $E = 23.66$ GPa, $\nu = 0.242$, $\sigma_{UCS} = 71.2$ MPa were obtained by Yang's method, and the corresponding relative error between numerical model and indoor sample are 17.1%, 7.6% and 11.3% respectively. The main cause of the error comes from the variations of rock properties. The obtained quantitative relationships (Eqs. (15)-(17)) are empirical in nature. It is difficult to calibrate the micromechanical parameters of a random rock only using the empirical relationships. Therefore, to reduce the error, Yang (2006) proposed that some modifications may be needed to model a specific material.

Zhou (2011) applied BP neural network model to inverse the micromechanical parameters. When the quantitative relationship between macro-micro parameters is not clear, it is appropriate to use neural network to realize the nonlinear mapping of macro-micro parameters.

When BP neural network is used for the

micromechanical parameter calibration, the approximation and generalization ability of BP neural network is closely related to the typicality of the samples. However, as a natural product, different diagenetic conditions endow the rock with different macro mechanical properties, even if the same rock may show great differences in macroscopic behaviors. Nevertheless, the BP neural network is still a feasible and effective method to calibrate the micromechanical parameters.

The comparison of relative errors using CM-LPBM and other calibration methods were shown in Fig. 10. It can be seen that the new calibration method, CM-LPBM, has higher accuracy. The proposed iterative correction formulas of micromechanical parameters can be used for compensating the relative error when semi-quantitative functional relationship is adopted to calibrate the micromechanical parameters of a specific rock. Thus the CM-LPBM overcomes the limitation of the application scope of Yang's method. Additionally, the proposed method is presented as a flow chart (see in Fig. 8), which has advantages of objectivity and efficiency compared with conventional "trial-and-error" method.

6. Conclusions

The main micromechanical parameters that affect the macroscopic mechanical parameters were revealed in present study. The semi-quantitative function relationships between the micromechanical parameters and the macroscopic parameters were established. Additionally, the iteration correction formula of the micromechanical parameters were proposed. An efficient calibration method for rock micromechanical parameters of parallel bond model (CM-LPBM) was developed, with the following conclusions.

(1) Based on the numerical simulation results and the multi-factor variance analysis, the independent micromechanical parameters of the LPBM to be calibrated were simplified to effective modulus, stiffness ratio, parallel bond normal strength and frictional coefficient.

(2) The semi-quantitative functional relationship between the macro-and micromechanical parameters using regression analysis was established. The iterative correction formula of the micromechanical parameters based on the single factor analysis was proposed.

(3) Laboratory experiment for the case study was carried out to verify the proposed calibration method (CM-LPBM). Using the proposed CM-LPBM, the micromechanical parameters of limestone were obtained by a few times of inversion calculation, which forms a sharp contrast compared to the traditional "trial-and-error" method. The error of macroscopic parameters between the numerical model and the indoor sample was less than 5%. The results show that the proposed parameter calibration method is efficient and reliable.

Acknowledgments

The research described in this paper was financially

supported by the National Natural Science Foundation of China (Grant No.: 51879153), the Natural Science Foundation of Shanodng Province (Grant No.: ZR201808080053) and the China Postdoctoral Science Foundation (Grant No.: 2019M662361).

References

- Ajamzadeh, M.R., Sarfarazi, V., Haeri, H. and Dehghani, H. (2018), "The effect of micro parameters of PFC software on the model calibration", *Smart Struct. Syst.*, **22**(6), 643-662. <https://doi.org/10.12989/sss.2018.22.6.643>.
- Bahaaddini, M., Hagan, P., Mitra, R. and Hebblewhite, B.K. (2016), "Numerical study of the mechanical behavior of nonpersistent jointed rock masses", *Int. J. Geomech.*, **16**(1), 1-10. [https://doi.org/10.1061/\(ASCE\)GM.1943-5622.0000510](https://doi.org/10.1061/(ASCE)GM.1943-5622.0000510).
- Bahaaddini, M., Sharrock, G. and Hebblewhite, B.K. (2013), "Numerical direct shear tests to model the shear behaviour of rock joints", *Comput. Geotech.*, **51**, 101-115. <https://doi.org/10.1016/j.compgeo.2013.02.003>.
- Bahrani, N. and Kaiser, P.K. (2017), "Estimation of confined peak strength of crack-damaged rocks", *Rock Mech. Rock Eng.*, **50**(2), 309-326. <https://doi.org/10.1007/s00603-016-1110-1>.
- Bock, S. and Prusek, S. (2015), "Numerical study of pressure on dams in a backfilled mining shaft based on PFC3D code", *Comput. Geotech.*, **66**, 230-244. <https://doi.org/10.1016/j.compgeo.2015.02.005>.
- Chen, Q., Zhang, C., Yang, C., Ma, C. and Pan, Z. (2019), "Effect of fine-grained dipping interlayers on mechanical behavior of tailings using discrete element method", *Eng. Anal. Boundary Elem.*, **104**, 288-299. <https://doi.org/10.1016/j.engabound.2019.03.029>.
- Cundall, P.A. and Strack, O.D.L. (1979), "Discrete numerical model for granular assemblies", *Geotechnique*, **29**(1), 41-65. <https://doi.org/10.1680/geot.1979.29.1.47>.
- De Silva, V.R.S. and Ranjith, P.G. (2020), "A study of rock joint influence on rock fracturing using a static fracture stimulation method", *J. Mech. Phys. Solids*, **137**, 21. <https://doi.org/10.1016/j.jmps.2019.103817>.
- Gracia, F., Villard, P. and Richefeu, V. (2019), "Comparison of two numerical approaches (DEM and MPM) applied to unsteady flow", *Comput. Particle Mech.*, **6**(4), 591-609. <https://doi.org/10.1007/s40571-019-00236-1>.
- Guo, W.B., Hu, B., Cheng, J.L. and Wang, B.F. (2020), "Modeling time-dependent behavior of hard sandstone using the DEM method", *Geomech. Eng.*, **20**(6), 517-525. <https://doi.org/10.12989/gae.2020.20.6.517>.
- Haeri, H., Sarfarazi, V., Zhu, Z.M. and Moosavi, E. (2019), "Effect of transversely bedding layer on the biaxial failure mechanism of brittle materials", *Struct. Eng. Mech.*, **69**(1), 11-20. <https://doi.org/10.12989/sem.2019.69.1.011>.
- Haeri, H., Sarfarazi, V., Zhu, Z.M. and Nejati, H.R. (2019), "Numerical simulations of fracture shear test in anisotropy rocks with bedding layers", *Adv. Concrete Construct.*, **7**(4), 241-247. <https://doi.org/10.12989/acc.2019.7.4.241>.
- Hasanpour, R., Ozcelik, Y., Yilmazkaya, E. and Sohrabian, B. (2016), "DEM modeling of a monowire cutting system", *Arab. J. Geosci.*, **9**(20), 11. <https://doi.org/10.1007/s12517-016-2710-5>.
- Hashemi, S.S., Momeni, A.A. and Melkoumian, N. (2014), "Investigation of borehole stability in poorly cemented granular formations by discrete element method", *J. Petrol. Sci. Eng.*, **113**, 23-35. <https://doi.org/10.1016/j.petrol.2013.11.031>.
- Hofmann, H., Babadagli, T., Yoon, J.S., Blocher, G. and Zimmermann, G. (2016), "A hybrid discrete/finite element modeling study of complex hydraulic fracture development for enhanced geothermal systems (EGS) in granitic basements", *Geothermics*, **64**, 362-381. <https://doi.org/10.1016/j.geothermics.2016.06.016>.
- Jafri, T.H. and Yoo, H. (2018), "REV application in DEM analysis of non-vibrational rock splitting method to propose feasible borehole spacing", *Appl. Sci.*, **8**(3), 17. <https://doi.org/10.3390/app8030335>.
- Khazaei, C., Hazzard, J. and Chalaturnyk, R. (2015), "Damage quantification of intact rocks using acoustic emission energies recorded during uniaxial compression test and discrete element modeling", *Comput. Geotech.*, **67**, 94-102. <https://doi.org/10.1016/j.compgeo.2015.02.012>.
- Kwok, Y. and Bolton, M.D. (2010), "DEM simulations of thermally activated creep in soils", *Géotechnique*, **60**(6), 425-433. <https://doi.org/10.1680/geot.2010.60.6.425>.
- Lin, P., Li, S.C., Xu, Z.H., Wang, J. and Huang, X. (2019), "Water inflow prediction during heavy rain while tunneling through Karst fissured zones", *Int. J. Geomech.*, **19**(8), 04019093. [https://doi.org/10.1061/\(ASCE\)GM.1943-5622.0001478](https://doi.org/10.1061/(ASCE)GM.1943-5622.0001478).
- Lotidis, M.A., Nomikos, P.P. and Sofianos, A.I. (2019), "Numerical study of the fracturing process in marble and plaster hollow plate specimens subjected to uniaxial compression", *Rock Mech. Rock Eng.*, **52**(11), 4361-4386. <https://doi.org/10.1007/s00603-019-01884-8>.
- Manouchehrian, A., Sharifzadeh, M., Marji, M.F. and Gholamnejad, J. (2014), "A bonded particle model for analysis of the flaw orientation effect on crack propagation mechanism in brittle materials under compression", *Arch. Civ. Mech. Eng.*, **14**(1), 40-52. <https://doi.org/10.1016/j.acme.2013.05.008>.
- Mehranpour, M.H., Kulatilake, P., Ma, X.G. and He, M.C. (2018), "Development of new three-dimensional rock mass strength criteria", *Rock Mech. Rock Eng.*, **51**(11), 3537-3561. <https://doi.org/10.1007/s00603-018-1538-6>.
- Meidani, M., Meguid, M.A. and Chouinard, L.E. (2018), "Estimating earth loads on buried pipes under axial loading condition: Insights from 3D discrete element analysis", *Int. J. Geo-Eng.*, **9**(1), 5. <https://doi.org/10.1186/s40703-018-0073-3>.
- Potyondy, D. (2018), "Material-Modeling Support in PFC [fistPkg26]", Itasca Consulting Group, Inc., Minneapolis, Minnesota, U.S.A.
- Potyondy, D.O. and Cundall, P.A. (2004), "A bonded-particle model for rock", *Int. J. Rock Mech. Min. Sci.*, **41**(8), 1329-1364. <https://doi.org/10.1016/j.ijrmm.2004.09.011>.
- Poulsen, B.A., Adhikary, D. and Guo, H. (2018), "Simulating mining-induced strata permeability changes", *Eng. Geol.*, **237**, 208-216. <https://doi.org/10.1016/j.enggeo.2018.03.001>.
- Sarfarazi, V., Haeri, H., Shemirani, A.B., Zhu, Z.M. and Marji, M.F. (2018), "Experimental and numerical simulating of the crack separation on the tensile strength of concrete", *Struct. Eng. Mech.*, **66**(5), 569-582. <https://doi.org/10.12989/sem.2018.66.5.569>.
- Shemirani, A.B., Haeri, H., Sarfarazi, V., Akbarpour, A. and Babanouri, N. (2018), "The discrete element method simulation and experimental study of determining the mode I stress-intensity factor", *Struct. Eng. Mech.*, **66**(3), 379-386. <https://doi.org/10.12989/sem.2018.66.3.379>.
- Shi, C., Yang, W., Yang, J. and Chen, X. (2019), "Calibration of micro-scaled mechanical parameters of granite based on a bonded-particle model with 2D particle flow code", *Granul. Matter*, **21**(2), 38. <https://doi.org/10.1007/s10035-019-0889-3>.
- Wu, X.J. (2017), "Study on mechanism of seepage and water-inrush from filled Karst conduit in tunnel", China University of Mining and Technology, Beijing, China.
- Xu, Z.H., Huang, X., Li, S.C., Lin, P., Shi, X.S. and Wu, J. (2020a), "A new slice-based method for calculating the minimum safe thickness for a filled-type karst cave", *Bull. Eng.*

- Geol. Environ.*, **79**(2), 1097-1111.
<https://10.1007/s10064-019-01609-9>.
- Xu, Z.H., Lin, P., Xing, H.L. and Wang, J. (2020b), "Mathematical modeling of cumulative erosion ratio for suffusion in soils", *Proc. Inst. Civ. Eng. Geotech. Eng.*, 1-11.
<https://doi.org/10.1680/jgeen.19.00082>.
- Xu, Z.H., Wang, W.Y., Lin, P., Wang, X.T. and Yu, T.F. (2020c), "Buffering effect of overlying sand layer technology for dealing with rockfall disaster in tunnels and a case study", *Int. J. Geomech.*, **20**(8), 04020127. [https://10.1061/\(ASCE\)GM.1943-5622.0001751](https://10.1061/(ASCE)GM.1943-5622.0001751).
- Yang, B., Yue, J. and Lei, S. (2006), "A study on the effects of microparameters on macroproperties for specimens created by bonded particles", *Eng. Comput.*, **23**(6), 607-631.
<https://doi.org/10.1108/02644400610680333>.
- Zhou, Y., Wu, S., Jiao, J. and Zhang, X. (2011), "Research on mesomechanical parameters of rock and soil mass based on BP neural network", *Rock Soil Mech.*, **32**(12), 3821-3826.
<https://doi.org/10.16285/j.rsm.2011.12.010>.